Oxygen-Assisted Charge Transfer Between ZnO Quantum Dots and Graphene

*Wenhao Guo, Shuigang Xu, Zefei Wu, Ning Wang, M. M. T. Loy, and Shengwang Du**

Graphene, consisting of sp^2 hybridized C-C bonds in a honeycomb-like two-dimensional network, is a promising material and platform for new types of optoelectronic devices and sensors because of its high carrier mobility, ultra stability and easy fabrication technique.[1–9] In this work, we demonstrate an efficient charge transfer between ZnO quantum dots (QDs) and a single layer graphene. We fabricate a graphene-based ultraviolet (UV) sensitive device with ZnO QDs on top of the graphene layer, and find that the electrical response of the device to UV light is largely enhanced due to the charge transfer. We show that the oxygen molecules play a vital role in the charge transfer process, by being adsorbed on or desorbed off the QDs surface. With a gain of as high as 10^7, this new hybrid nano structure may lead to the improvements for design of the photoelectric devices and the realization of high performance graphene-based UV sensors and detectors.

Although graphene has many fascinating optical and electrical properties, its relative low light absorption coefficient[10] and too fast recombination rate[11] have limited pristine graphene from practical optoelectronic applications. Recently, considerable attention has been attracted to adding active components on top of the pristine graphene device to improve its performance and develop new functional applications. Among these, semiconductor QDs, with their strong light absorption and good compatibilities, have arose intense interests.[12–23] Combining the photo-induced charge separation ability of QDs and the electronic transport property of graphene, it is possible to make these hybrid structures remarkable candidates for novel optoelectronic devices. Therefore, a deep understanding of the interaction between QDs and graphene will be beneficial to design and manufacture practical products. Up to date, while many studies have focused on the properties of the device under infrared and visible light illumination, only few efforts have been put on investigating the detailed interaction mechanism of the hybrid structure with the irradiation of UV light, which is important for potential applications in UV-related optoelectronic devices. Consequently, ZnO QDs, chosen for their large bandgap (about 3.3 eV), would allow us to focus on the device response to UV light and screen the influence from visible and infrared light source.

Figure 1a,b illustrate the schematics of our fabricated graphene device decorated with ZnO QDs. We mechanically exfoliate single layer graphene onto silicon dioxide (300 nm in thickness) on a degenerately doped silicon wafer. The size of graphene is about 10 μm × 30 μm. The electrodes are patterned through conventional electron beam lithography and deposited by Ti/Au electrodes through thermal evaporation. For the following measurement, as shown in Figure 1b, source-drain voltage (V_{DS}) was applied between the source and drain electrodes, and gate voltage (V_G) was applied between the drain electrode and the silicon layer. It is noteworthy that when exposed to the air environment, there would be amount of oxygen molecules adsorbed on the surface of the device. ZnO QDs were made by hydrothermal methods, dissolved in methanol, and then sprayed onto the device by airbrush. The high-resolution transmission electron microscopy (HRTEM) image and electron diffraction pattern are displayed in Figure 1c and d, respectively. The QDs, with a diameter of about 3–5 nm and fine structural integrity, are of good qualities.

We first measured the resistance-to-gate-voltage transport properties of the pristine graphene without ZnO QDs. To eliminate possible artifacts from the gate hysteresis, all of the resistance-voltage curves were acquired on the same measurement cycle while we scanned the bias from positive to negative values. As we see in **Figure 2**a, the charge neutrality point (CNP) was initially at 18 V, shown by curve 1, due to the doping effects from the air and substrate. After we placed ZnO QDs on the device, the CNP was shifted to about 8 V, as shown by curve 2, consistent with a slightly higher working function of ZnO QDs compared to graphene, and the carrier mobility was slightly decreased from 3600 $cm^2V^{-1}s^{-1}$ to 3000 $cm^2V^{-1}s^{-1}$ due to the disorder introduced by the QDs.

We then put the device in the chamber of near-field scanning optical microscope (NSOM) at the ambient environment to investigate its optoelectronic properties when exposed to UV light. A cantilevered fiber probe was used to couple the laser beam to illuminate the sample. The beam spot was adjusted large enough to cover the area of graphene. 325 nm He-Cd laser (Melles Griot, 54 series) was

W. Guo, S. Xu, Z. Wu, Prof. N. Wang, Prof. M. M. T. Loy, Prof. S. Du
Department of Physics
The Hong Kong University of Science and Technology
Clear Water Bay, Kowloon, Hong Kong, China
E-mail: dusw@ust.hk

DOI: 10.1002/smll.201202855

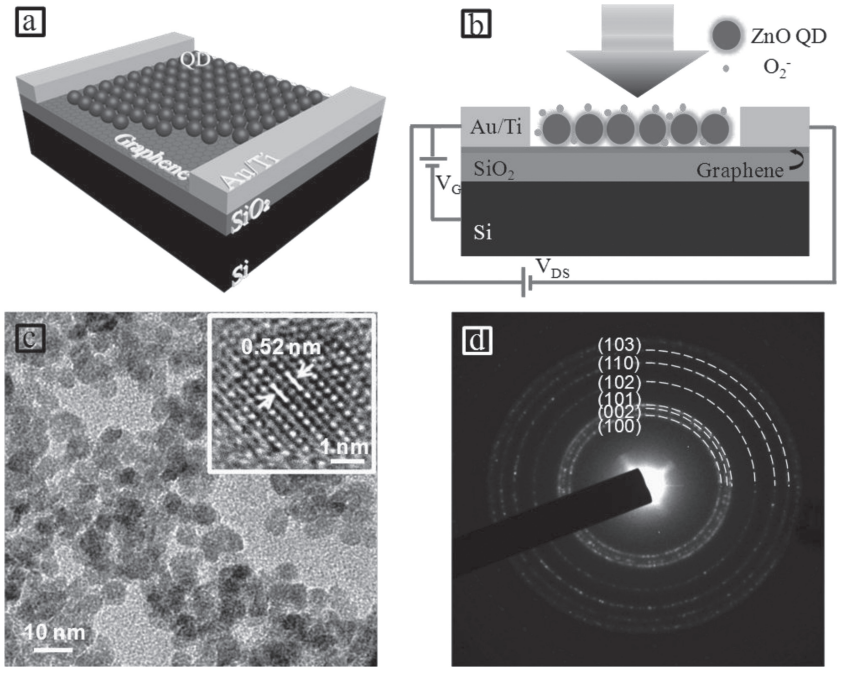

Figure 1. (a) Schematics of the graphene device coated with ZnO QDs; (b) Side view of the device; (c) HRTEM image and (d) electron diffraction pattern of the ZnO QDs.

used to shine on the device, with the excitation intensity 100 $mWcm^{-2}$. As curve 3 in Figure 2a shows, when the laser is on, the CNP moves to about –40 V, indicating that the electrons are transferred to graphene due to the UV irradiation. This is opposite to the holes transfer mechanism observed from other groups.[21,22,24] After we remove the excitation laser, as no more electron-hole pairs are generated, the CNP returns to about 10 V, illustrated by curve 4.

We have also taken an AFM image of our device after ZnO QDs were sprayed on graphene, see Figure S1 in Supporting Information. It turns out ZnO QDs form many discrete islands with thickness of several tens of nanometers, which may be due to the aggregation of the ZnO QDs. Using the same spray method, we made a control device of ZnO QDs alone to investigate its optoelectrical properties. In the dark condition, the resistance is more than 10^{10} Ohms. When we shine 325 nm laser on the device, this resistance value doesn't change at all. This result confirms that the electronic transportation properties we measured for the hybrid structures are indeed mainly from graphene, not from the pure QDs. Meanwhile, the transport characteristics of our device in Figure 2a are the typical graphene ambipolar field effect, which is very different from the n-type semiconductor behavior in ZnO QDs.[25]

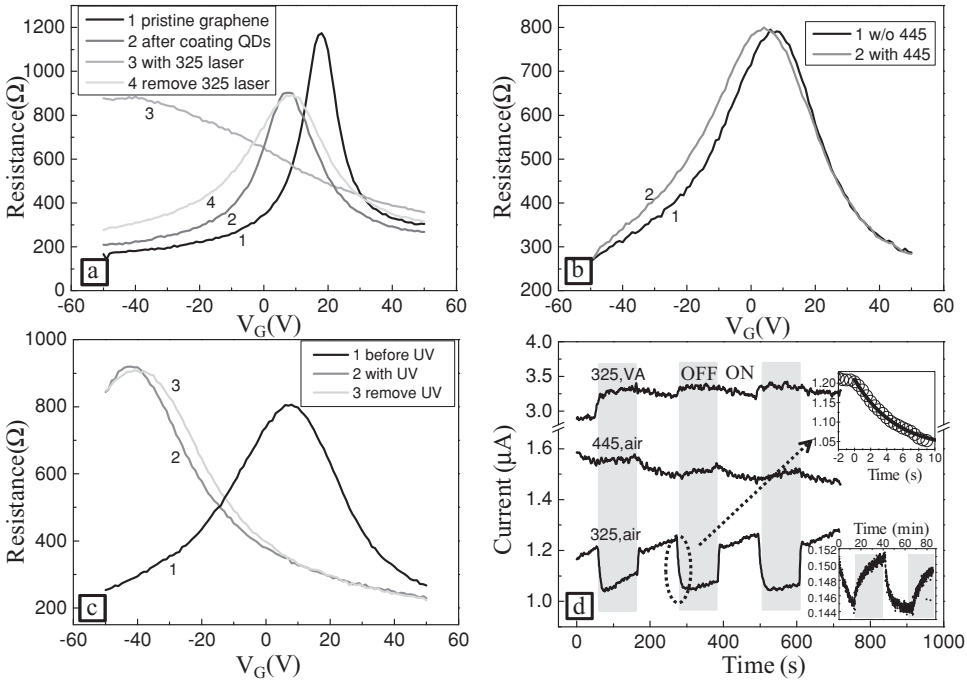

Figure 2. (a) Transport measurements of pristine graphene, graphene/ZnO QDs, with 325 nm laser illumination, removal the 325 nm laser, respectively; (b) Transport measurements of graphene/ZnO QDs with and without 445 nm laser illumination; (c) Transport measurement of graphene/ZnO QDs in the vacuum condition (10^{-6} mbar) with and without 325 nm laser illumination. (d) Graphene/ZnO QDs electrical response to the light on/off under three cases: in the air, with and without 325 nm laser; in the air, with and without 445 nm laser; in the vacuum, with and without 325 nm laser, respectively. The time interval between light on/off was 120 s. The top inset shows the exponential decay fit for the falling edge of the photocurrent when we turn off the light. The bottom inset shows pristine graphene electrical response to 325 nm laser on/off in the air. All the measurements were conducted with V_{DS} = 1 mV.

NANO MICRO small

As a control experiment, we repeat the measurement for the hybrid ZnO QDs/graphene device with 445 nm illumination. The excitation intensity was also 100 mWcm^{-2}. In this case, no electron-hole pair would be generated because the bandgap of ZnO QDs was higher than the energy of excitation photons. Therefore there would be no electron transfer process occurring at the QD/graphene interface. It is confirmed by the transport curve (curve 1 for without 445 nm laser illumination, curve 2 for with 445 nm laser illumination) in Figure 2b, where no clear shift of CNP is observed.

It has been proposed that oxygen molecules can grab the electrons from the n-type metal oxide semiconductors, adsorb on their surface, and thus change the carrier densities.[26] To better understand the charge transfer mechanism of the device, we put the sample in vacuum (VA) conditions (10^{-6} mbar). Figure 2c illustrates that under the vacuum condition, with 325 nm light irradiation, the CNP of graphene undergoes a significant shift towards about –40 V because of electron transfer, as shown in curve 2. However, it does not return after we switch off the laser, shown by curve 3. To further confirm the results, we have also done the control experiments in both nitrogen and oxygen environment, see Figure S2 in Supporting Information. In nitrogen, similar to the vacuum case, the UV light causes a left shift of CNP, and the CNP would not come back after we switch off the UV light; while in oxygen, it resembles the case in the air, the CNP would undergo a left shift with irradiation of UV light, and come back to its original place after we remove the UV light. We therefore believe that oxygen molecules play an important role in this electron transfer process, because in the vacuum condition the oxygen molecules are pumped away after the UV induced desorption.

Once the electrons of ZnO QDs are transferred to graphene, they can recirculate in the graphene channel within the lifetime. If the lifetime is long enough, it forms a gain system which could be utilized as highly sensitive light detectors or sensors. To determine the lifetime of the transferred electrons, we switched on and off the laser alternatively to measure the changes in the electronic characteristics. All the measurements are conducted at $V_G = 0$ V to remove the artifacts of the gate-voltage introduced molecule adsorption/desorption.[27] The source-drain voltage V_{DS} is set to be 1 mV. As shown in Figure 2d, when the device is exposed to air, during UV light irradiation (325, air), an increase of the source-drain current is observed, confirming that electrons were transferred from the QDs to graphene. After the UV light is switched off, the current drops to its original level. From the falling edge of the curve, we get the carriers' lifetime τ by fitting it with an exponential function $\exp(-t/\tau)$ and obtain τ = 5 s, as shown in the top inset in Figure 2d. This approach has been widely used and proved to be an efficient way to determine the carriers' lifetime.[21,22,26] Then we put the device in the vacuum condition with 325 nm laser irradiation (325, VA), and in air with 445 nm laser (445, air). As expected, the device has no noticeable response when we switch on and off the light, as shown in Figure 2d.

For comparison, the electronic response of pristine graphene in air has also been investigated, as shown in the bottom inset of Figure 2d. The UV irradiation results in light-induced desorption of small molecules from graphene and make it weakly p-doped. When the UV light is turned off, the small molecules would re-adsorb on graphene's surface.[28] This process changes the local carrier concentration and leads to significant variation in resistance. The desorption and adsorption processes typically have long time constants of hundreds of seconds, which is consistent with our experimental result in Figure 2d: the electronic response was very slow (the 325 nm laser on/off period was 20 minutes in this case). This desorption and re-adsorption of dopants on the surface of graphene differ from the charge transfer process which occurs in a much short time scale (τ = 5 s).

Now it becomes clear that coating with ZnO QDs helps graphene get a faster response to UV light from tens of minutes to several seconds, as a result of electron transfer between the QDs and graphene with assistance from the oxygen molecules in air. Our model of such charge transfer mechanism is illustrated schematically in **Figure 3**a–d. For semiconductor QDs, there is a high density of hole-trap states on the QD surface due to the high surface-to-volume ratio, with exposure to the air environment. For ZnO, it has been known that,[29–33] oxygen molecules can be adsorbed on the oxide surface and capture the free electrons present in the n-type metal oxide semiconductors, $[O_2(g) + e^- \rightarrow O_2(ad)]$. Under irradiation with photon energy larger than the bandgap, electron-hole pairs are generated (Figure 3a) and soon separated, with the holes trapped at the surface along the potential slope due to the band bending, leaving behind unpaired electrons (Figure 3b). The holes therefore discharge the adsorbed oxygen ions, $[O_2(ad) + h^+ \rightarrow O_2(g)]$, and the neutral oxygen molecules are then desorbed from the surface, as shown in Figure 3b. Following the energy diagram in Figure 3e, the electrons are transferred to graphene layer and raise the Fermi energy level, which leads to the left-shift of CNP of graphene. With shining UV light for sufficient long time, these processes reach equilibrium. Afterwards, when the UV light is switched off, if there are plenty of oxygen molecules surrounding, they will be re-adsorbed on the QDs' surface and capture the electrons, hence lower the Fermi energy level, and the transport properties of graphene will be recovered. If there are no oxygen molecules left (such as in the vacuum condition), the Fermi energy level will stay unchanged, and the CNP of graphene will not return to its original value. This charge transfer mechanism can be used for applications in such as UV detectors and sensors, given that the device has relative quick response at ambient conditions.

One important parameter to characterize the performance of an optoelectronic sensor is the responsivity. To study the responsivity of this hybrid structure, we express the density of free carriers (N) in the QDs[26] as

$$N = \frac{\eta P}{h\nu} T(P) \quad (1)$$

where η is the charge carrier photogeneration quantum efficiency, P is excitation laser intensity, $h\nu$ is the energy of incident photons, and T is the carrier lifetime. We have measured the photocurrent I_{ph} (calculated as I_{light}–I_{dark}) with different

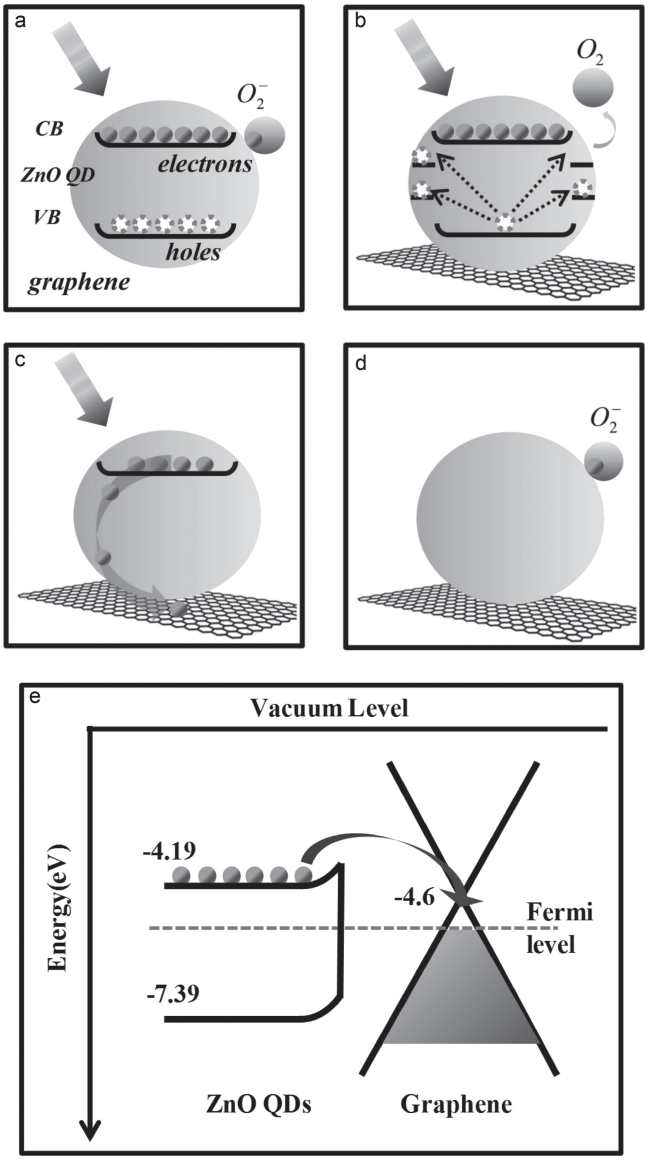

Figure 3. The mechanism of the oxygen-assisted charge transfer process. (a) With irradiation of photon energy larger than the bandgap of the QDs, electron-hole pairs are generated. (b) The holes are trapped at the surface states, leaving behind the unpaired electrons. The trapped holes will discharge the oxygen ions on the surface, and the oxygen molecules are desorbed. (c) The electrons will transfer from the QDs to the graphene layer. (d) With laser turned off, no more electron-hole pairs are generated. The oxygen molecules will re-adsorb on QDs and capture the remaining electrons to form oxygen ions on the surface. (e)The energy diagram of ZnO QDs and graphene.

intensities of UV light illumination. At low intensity excitation, the holes, separated from photon-introduced electron-hole pairs, occupy the surface states, thus are trapped at the surface and discharge the adsorbed oxygen molecules. As we increase the excitation light intensity, more and more electron-hole pairs are generated. After all the surface states are filled, the extra electron-hole pairs recombine immediately after they are generated, in the time scale of several tens of picoseconds.[34] Thus, they will not participate in the charge transfer process, and the average lifetime will be shortened. The excitation-intensity-dependant carrier lifetime can be expressed as

$$T(P) = T_0 \frac{1}{1 + (P/P_0)^n} \tag{2}$$

Here, T_0 is the carrier lifetime at low excitation intensity ($P \to 0$). P_0 is the excitation intensity in which the surface states are fully filled and n is a phenomenological fitting parameter. Taking advantages of the high carrier mobility in graphene, the transferred electrons can recirculate between the source and drain electrodes for many times within the long lifetime, resulting in a relative high gain and responsivity. The gain of the system is defined as the ratio between the number of electrons recirculated per unit time and the number of photons absorbed per unit time. The photocurrent (I_{ph}) takes the usual form as

$$I_{ph} = \alpha q N v W = \frac{\alpha q \eta W L}{h\nu} \left(\frac{T_0}{T_t}\right) \frac{P}{1 + (P)\, P_0)^n} \tag{3}$$

where α is the carrier transfer efficiency from ZnO QDs to graphene, q is the elementary charge, W is the sample width, and $v = \mu V_{DS} L^{-1}$ is the carrier drift velocity in graphene with the carrier mobility μ and the sample length L. $T_t = L^2 \mu^{-1} V^{-1}$ is the carrier transit time. In our work, with W = 30 μm, L = 10 μm, V_{DS} = 1 mV, and μ = 3000 cm$^2 V^{-1} s^{-1}$, T_t is estimated to be 330 ns. Assuming η = 1 and α = 1,[26] we estimate the gain by

$$G = \frac{I_{ph} h\nu}{q\, P\, W L} = \left(\frac{T_0}{T_t}\right) \frac{1}{1 + (P)\, P_0)^n} \tag{4}$$

Figure 4 shows the gain as a function of excitation intensity, as compared to the theory. The solid curve is the best fitting with $P_0 = 3.91 \times 10^{-8}$ Wcm^{-2} and n = 1.05. Our data agrees well with the theory at relative high excitation intensity, showing a high gain up to 10^4. And the responsivity of the device is calculated to be in the order of 10^4 AW^{-1}, with the excitation intensity as low as 10^{-5} Wcm^{-2}. At a lower excitation intensity ($P \to 0$), we predict the gain can be as high as 10^7. To compare with the performance of ZnO nanowire

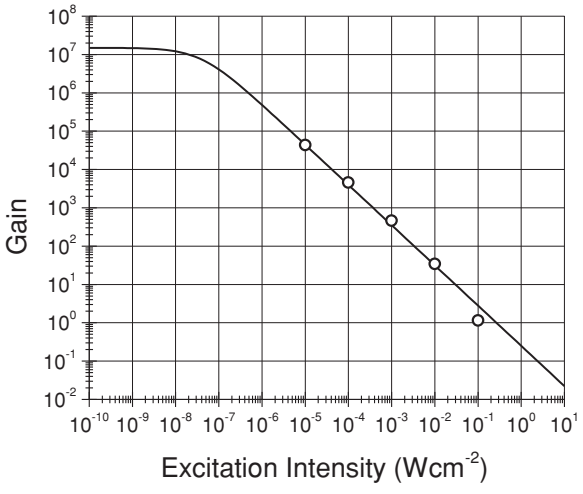

Figure 4. Gain as a function of excitation intensity. The circles are experimental data, and the solid curve is the theoretical plot with best fitting.

NANO MICRO small

device,[26] the advantage of our hybrid ZnO QDs/graphene device is that if put under the same condition, such as the same sample length, the same bias voltage, our device could reach a higher gain, due to the higher mobility of carriers in graphene than in ZnO nanowires. Usually, it could be two orders higher. Besides this, since graphene has much lower resistance than ZnO nanowire, our device can work at lower bias and have much less energy consumption.

In summary, we have investigated the oxygen-assisted charge transfer mechanism between ZnO QDs and graphene. With UV light illumination, after the generation of electron-hole pairs, the holes are separated and trapped into the surface states, and discharge the oxygen ions adsorbed on the surface of QDs. The unpaired electrons are then transferred to the graphene layer with a relative long lifetime. After the UV light is switched off, the oxygen molecules re-adsorb to the QDs surface, capture electrons and recover the graphene's transport properties. This ZnO QDs/graphene hybrid structure also shows a photoconductive gain as high as 10^7, which can be utilized for practical graphene-based UV sensors and detectors with very high responsivity. And this gain can be further enhanced by another 2-3 orders by increasing source-drain voltage, shortening the sample's length, etc.[22]

Experimental Section

Materials: Graphene was exfoliated from graphite by mechanical cleavage onto degenerately doped Si substrates with 300 nm SiO_2. ZnO QDs were prepared according to the method of Pacholski.[35] Typically, 65 mL KOH solution in methanol (0.03 M) was added drop by drop to 125 mL solution of zinc acetate dehydrate (0.01 M) in methanol at 60 °C and stirred for two hours. The resulting milky precipitate was collected and washed with methanol several times. Then the product was redispersed in methanol for storage. The structure of ZnO QDs was characterized by transmission electron microscopy (TEM, JEOL 2010F).

Device Fabrication: The electrical contacts of graphene were patterned by standard electron-beam lithography and the electrodes were deposited with 5 nm Ti and 40 nm Au using electron-beam deposition, followed by lift-off process. After the characterization of the pristine graphene, the ZnO QDs were sprayed on top of graphene device using an airbrush.

Electrical Characterization: The electrical transport and optical response of the devices were carried out in the chamber of NSOM. The resistance-gate voltage characteristics of devices were measured using standard lock-in techniques. For the optical response of the devices, 325 nm and 445 nm lasers were used as the light source. The measurements of dark current and photocurrent were carried out by Keithley 6430.

Supporting Information

Supporting Information is available from the Wiley Online Library or from the author.

Acknowledgements

The authors thank K.S. Wong for providing the laser for the control experiments. The work was supported by the Hong Kong Research Grants Council under the project Nos. N_HKUST613/12, 604112, HKUST9/CRF/08, and HKU8/CRF/11G. The technical support of the Raith-HKUST Nanotechnology Laboratory for the electron-beam lithography facility (Project No. SEG HKUST08) are hereby acknowledged.

[1] F. Bonaccorso, T. Sun, Z. Hasan, A. C. Ferrari, *Nat. Photon.* **2010**, *4*, 611.
[2] Jiwoong. Park, Y. H. Ahn, Carlos. Ruiz-Vargas, *Nano Lett.* **2009**, *9*, 1742.
[3] F. Xia, T. Mueller, R. Golizadeh-Mojarad, M. Freitag, Y.-m. Lin, J. Tsang, V. Perebeinos, P. Avouris, *Nano Lett.* **2009**, *9*, 1039.
[4] F. Xia, T. Mueller, Y.-m. Lin, A. Valdes-Garcia, P. Avouris, *Nat. Nanotechnol.* **2009**, *4*, 839.
[5] A. K. Geim, K. S. Novoselov, *Nat. Mater.* **2009**, *6*, 183.
[6] A. K. Geim, *Science* **2009**, *324*, 1530.
[7] C. N. R. Rao, A. K. Sood, K. S. Subrahmanyam, A. Govindaraj, *Angew. Chem. Int. Ed.* **2009**, *48*, 7752.
[8] T. Yamada, R. Kumai, Y. Takahashi, T. Hasegawa, *J. Mater. Chem.* **2010**, *20*, 5810.
[9] D. Wei, Y. Liu, *Adv. Mat.* **2010**, *22*, 3225.
[10] R. R. Nair, P. Blake, A. N. Grigorenko, K. S. Novoselov, T. J. Booth, T. Stauber, N. M. R. Peres, A. K. Geim, *Science* **2008**, *320*, 1308.
[11] J. M. Dawlaty, S. Shivaraman, M. Chandrashekhar, F. Rana, M. G. Spencer, *Appl. Phys. Lett.* **2008**, *92*, 042116.
[12] X. Geng, L. Niu, Z. Xing, R. Song, G. Liu, M. Sun, G. Cheng, H. Zhong, Z. Liu, Z. Zhang, L. Sun, H. Xu, L. Lu, L. Liu, *Adv. Mater.* **2010**, *22*, 638.
[13] Y. Lin, K. Zhang, W. Chen, Y. Liu, Z. Geng, J, . Zeng, N. Pan, L. Yan, X. Wang, J. G. Hou, *ACS Nano* **2010**, *4*, 3033.
[14] A. Cao, Z. Liu, S. Chu, M. Wu, Z. Ye, Z. Cai, Y. Chang, S. Wang, Q. Gong, Y. Liu, *Adv. Mater.* **2010**, *22*, 103.
[15] X. Yang, X. Zhang, Y. Ma, Y. Huang, Y. Wang, Y. Chen, *J. Mater. Chem.* **2009**, *19*, 2710.
[16] J. Chu, X. Li, P. Xu, *J. Mater. Chem.* **2011**, *21*, 11283.
[17] K. K. Manga, S. Wang, M. Jaiswal, Q. Bao, K. P. Loh, *Adv. Mater.* **2010**, *22*, 5265.
[18] G. Williams, B. Seger, P. V. Kamat, *ACS Nano* **2008**, *2*, 1487.
[19] H. Yang, G. H. Guai, C. Guo, Q. Song, S. P. Jiang, Y. Wang, W. Zhang, C. M. Li, *J. Phys. Chem. C* **2011**, *115*, 12209.
[20] H. Wang, L.-F. Cui, Y. Yang, H. S. Casalongue, J. T. Robinson, Y. Liang, Y. Cui, H. Dai, *J. Am. Chem. Soc.* **2010**, *132*, 13978.
[21] Z. Sun, Z. Liu, J. Li, G.-a. Tai, S.-P. Lau, F. Yan, *Adv. Mater.* **2012**, *24*, 5878.
[22] G. Konstantatos, M. Badioli, L. Gaudreau, J. Osmond, M. Bernechea, F. P. Garcia de Arquer, F. Gatti, F. H. L. Koppens, *Nat. Nanotechnol.* **2012**, *7*, 363.
[23] D. Zhang, L. Gan, Y. Cao, Q. Wang, L. Qi, X. Guo, *Adv. Mat.* **2012**, *24*, 2715.
[24] Q. Wang, X. Guo, L. Cai, Y. Cao, L. Gan, S. Liu, Z. Wang, H. Zhang, L. Li, *Chem. Sci.* **2011**, *2*, 1860.
[25] Y. Jin, J. Wang, B. Sun, J. C. Blakesley, N. C. Greenham, *Nano Lett.* **2008**, *8*, 1649.
[26] C. Soci, A. Zhang, B. Xiang, S. A. Dayeh, D. P. R. Aplin, J. Park, X. Y. Bao, Y. H. Lo, D. Wang, *Nano Lett.* **2007**, *7*, 1003.
[27] Y. Sato, K. Takai, T. Enoki, *Nano Lett.* **2011**,*11*, 3468.
[28] P. Sun, M. Zhu, K. Wang, M. Zhong, J. Wei, D. Wu, Y. Cheng, H. Zhu, *Appl. Phys. Lett.* **2012**, *101*, 053107.
[29] H. Kind, H. Yan, B. Messer, M. Law, P. Yang, *Adv. Mater.* **2002**, *14*, 158.

[30] J. B. K. Law, J. T. L. Thong, *Appl. Phys. Lett.* **2006**, *88*, 133114.
[31] Z. Fan, P. c. Chang, J. G. Lu, E. C. Walter, R. M. Penner, C. h. Lin, H. P. Lee, *Appl. Phys. Lett.* **2004**, *85*, 6128.
[32] Q. H. Li, T. Gao, Y. G. Wang, T. H. Wang, *Appl. Phys. Lett.* **2005**, *86*, 123117.
[33] S. Kumar, V. Gupta, K. Sreenivas, *Nanotechnology* **2005**, *16*, 1167.
[34] V. A. Fonoberov, A. A. Balandin, *J. Nanoelectron. Opote.* **2006**, *1*, 19.
[35] C. Pacholski, A. Kornowski, H. Weller, *Angew. Chem. Int. Ed.* **2002**, *41*, 1188.

Received: November 16, 2012
Revised: December 13, 2012
Published online: March 21, 2013

